Digital RFI Suppression in DMT-Based VDSL Systems

Frank Sjöberg, *Member, IEEE*, Rickard Nilsson, *Member, IEEE*, Per Ola Börjesson, *Senior Member, IEEE*, Per Ödling, *Senior Member, IEEE*, Brian Wiese, and John A. C. Bingham, *Life Fellow, IEEE*

***Abstract*—In this paper, we propose a method for suppressing radio frequency interference (RFI) in discrete multitone (DMT) based very high bit rate digital subscriber line (VDSL) systems. The method operates in the frequency domain of a DMT system. First, we derive a model of how an unknown narrow-band RF signal is mapped onto the DMT carriers. Then, by measuring the RFI on a few *unused* DMT carriers we are able to subtract RFI estimates from every *modulated* subcarrier. Simulation results show that this method, applied to an RFI signal with the same average power as the VDSL signal, suppresses the RFI with 40–50 dB, which reduces the average SNR loss from about 20 to less than 0.3 dB.**

***Index Terms*—Discrete multitone (DMT), radio frequency interference (RFI), subscriber loops, very high bit rate digital subscriber line (VDSL).**

I. Introduction

RADIO frequency (RF) signals transmitted in the vicinity of an unshielded twisted pair wire may cause radio frequency interference (RFI) with signals in the wire [1]. In this paper we address the problem of RFI in discrete multitone (DMT) [2] based very high bit rate digital subscriber line (VDSL) [3], [4] systems. We describe a method for suppressing the RFI signal in the frequency domain.

VDSL is the latest DSL technology standardized by the European Telecommunications Standards Institute (ETSI), the American National Standards Institute (ANSI), and the International Telecommunication Union (ITU-T). VDSL supports transmission rates of up to 52 Mb/s on unshielded twisted pair wires. To achieve these high bit rates, VDSL must use a large frequency band ranging from around 300 kHz up to 15 MHz. In this range, VDSL will share some frequency bands, known as HAM bands, with radio amateurs.

Manuscript received April 8, 2003; revised April 13, 2004. This paper was presented in part at the International Conference on Telecommunications, Porto Carras, Greece, June, 1998. This work was supported in part by the Austrian Kplus program. This paper was recommended by Associate Editor S.-M. Phoong.

F. Sjöberg is with the Division of Signal Processing, Luleå University of Technology, SE-971 87 Luleå, Sweden.

R. Nilsson is with the Telecommunications Research Center Vienna (ftw.), A-1220 Wien, Austria (e-mail: rickard.nilsson@ftw.at).

P. O. Börjesson and P. Ödling are with the Department of Information Technology, Lund Institute of Technology, SE-221 00, Lund, Sweden.

B. Wiese is with 2Wire Inc., San Jose, CA 95131, USA.

J. A. C. Bingham, retired, was with Texas Instruments Broadband Access Group, San Jose, CA 95124 USA. He is now at 2353 Webster St., Palo Alto, CA 94301-4056 USA.

Digital Object Identifier 10.1109/TCSI.2004.836865

Since the twisted pair wires are not shielded, two types of related problems will appear: RFI *ingress* and *egress*; i.e., the reception and radiation of radio signals into and out from the wire, respectively. In this paper, we consider the problem of RF ingress into VDSL systems. When a radio amateur transmits within a HAM band overlapping the VDSL spectrum, it will interfere with all DMT tones including those outside the HAM band (due to sidelobe leakage). Hence, to avoid a large performance degradation it is desirable to suppress the RFI as much as possible.

Earlier suggestions for suppressing the RFI include the use of an analog precanceller using common-mode (CM) to differential-mode (DM) conversion [5], adaptive mixed-signal narrow-band interference cancellation [6], and pulse shaping of the data symbols [7]. The latter we will refer to as *windowing*. By themselves these methods suppress the RFI to a certain extent but often not enough.

Other methods to achieve robustness against narrow-band interference include adaptive notch filtering [8] and using alternative filter banks [9] to the standard *discrete Fourier transform* (DFT), which is used for DMT–VDSL. However, steep notch filters that effectively suppress RFI also increase the length of the total channel impulse response, which may lead to intersymbol- and intercarrier interference in a DMT receiver. Alternative filter banks to the DFT can be designed to have less sidelobe leakage and better immunity against RFI, with a small penalty of nonperfect reconstruction, but they do not comply with the existing DFT-based DMT–VDSL standards.

By expanding an idea, introduced in [10], we develop an RFI cancelling method for DMT–VDSL which is capable of suppressing general (unknown) narrow-band RF signals. The number of parameters to be used, determining the complexity of the method, is a designer's choice. It depends on the bandwidth of the disturber and on if any windowing is used in the receiver. Following two system proposals, we will focus here on the case with windowing, resulting in a recommendation to use only two parameters [11] (see also, [12]), and [13].

Our method operates in the signal's frequency domain after the analog-to-digital converter (ADC) and after the DFT processor. When we analyze the RFI at each DMT tone, we consider a transfer function which maps the RF disturbance to the tones. Based on RFI measurements on a few *unused* tones, we extrapolate the RFI that is present on all *modulated* DMT tones. We safely assume that unused tones are always available as they have to be silent because of the egress problem.

RFI cancellation can be done with great accuracy as the RFI is very narrow-band. Simulation results show that our method

1057-7122/04$20.00 © 2004 IEEE

TABLE I
FIVE INTERNATIONAL AMATEUR RADIO BANDS OVERLAPPING VDSL SPECTRUM

Start (MHz)	1.81	3.50	7.00	10.10	14.00
Stop (MHz)	2.00	3.80	7.10	10.15	14.35

can suppress an RFI signal, with the same average power as the VDSL signal, from an average signal-to-noise ratio (SNR) loss of 20 down to less than 0.3 dB.

II. RFI

An unshielded twisted pair wire works as a CM antenna that both generates and receives radio signals in the VDSL systems' frequency range (from approximately 300 kHz up to 15 MHz). VDSL signals are transmitted and received as DM signals, but unbalance in the wire will cause CM/DM conversion [1], resulting in both RF ingress and RF egress.

The main source of RFI is believed to be amateur radio transmitters. This is because they can be located just a few meters from an unshielded wire [1] and the transmitting power is expected to be high—up to 400 W in the U.K. and 1.5 kW in USA. Radio amateurs are allowed to operate at certain frequencies, called the *HAM bands*, which are listed in Table I [14]. According to VDSL standardization, the systems are required to handle amateur radio signals with up to 4-kHz bandwidth.

III. SUPPRESSION OF RF INGRESS

Since the signal power of the RFI may be high, it may cause signal clipping in the ADC. To avoid this, an analog RFI canceller first has to suppress the RFI to the level of the desired signal [6]. However, the interference after the analog RFI canceller and the ADC can be severe and it is thus important to combat the RFI also in the digital domain. Fig. 1 shows a DMT system with an analog precanceller and a frequency-domain RFI canceller.

DMT tones in the HAM bands must be silent to avoid RF egress [5]. Our method measures the RF-disturbance on a few of the silent (unused) DMT tones in each HAM band and then subtracts estimates of any disturbance from the data-carrying tones. This idea was introduced in [10] for a sinusoid RF signal with known frequency. We now expand on this idea in two directions and develop a method for any narrow-band RF-disturbance with a roughly known centre frequency, which we also give strategies on how to estimate.

In this section, we develop a signal model of a received RF signal. The model describes how the RF signal interferes with each DMT tone in a DMT system. We parameterize the disturbance and estimate the unknown parameters using measurements from unused tones. Then, we calculate and finally subtract estimates of the disturbance from the data, see Fig. 2.

A. Signal Model

In this subsection, we derive the properties of the RFI in the DFT domain. This will be used in the subsequent derivation of the RFI canceller. Starting with the received signal expressed as

$$r(t) = x(t) + s(t) + n(t) \tag{1}$$

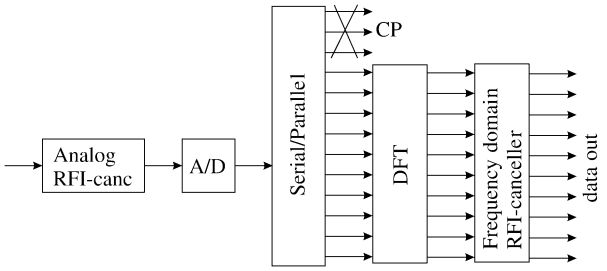

Fig. 1. DMT system with analog precanceller and the frequency-domain RFI canceller.

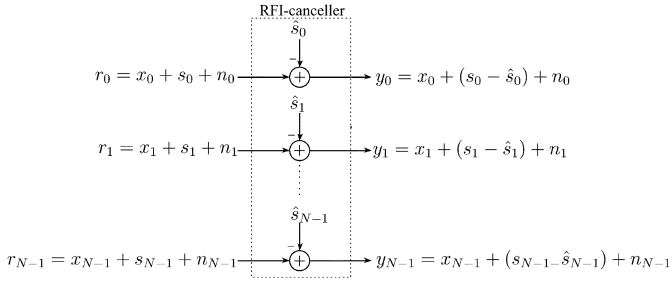

Fig. 2. Frequency-domain RFI canceller.

where $x(t)$ is the received baseband DMT signal, $s(t)$ is an unknown narrow-band RF signal, and $n(t)$ represents other noise sources such as *far-end crosstalk* (FEXT) and *additive white Gaussian noise* (AWGN). In Appendix B we give a specific narrow-band model of $s(t)$, that can represent any type of analog modulation, amplitude modulation, double sideband modulation, single sideband modulation (SSB), *etc.*

The RFI canceller works in the frequency domain, after the DFT. It is here that the importance of the windowing in the receiver is seen. (A sketch of how the windowing is performed is given in Appendix A.) Sampling and DFT-demodulation of the received signal $r(t)$ from (1) yields

$$r_k = \sum_{n=0}^{2N-1+\mu} w[n] r\left(\frac{n}{f_s}\right) e^{-j(2\pi kn/2N)} \tag{2}$$

$$= x_k + s_k + n_k, \qquad 0 \le k \le N-1 \tag{3}$$

where $w[\cdot]$ is the window used in the receiver, x_k is the received VDSL baseband signal after the DFT, s_k are the narrow-band RF signal's DFT coefficients, n_k is the DFT of the noise and f_s is the sampling frequency. If the DMT signal is cyclically extended with μ samples, the windowing will not destroy the subcarrier orthogonality of the DMT signal, i.e., the perfect reconstruction property of the DFT is preserved also when receiver windowing is performed. For this type of windowing operation we have in mind, a symmetrical window is therefore necessary [7], as described in Appendix A.

To cancel the interference s_k, we want to subtract an estimate, $\widehat{s}_k$, from (3)

$$r_k - \widehat{s}_k = x_k + (s_k - \widehat{s}_k) + n_k. \tag{4}$$

In order to derive the estimates $\widehat{s}_k$ we first set up the following relation between s_k and the Fourier transform of the disturbance $S(f) = \mathcal{F}\{s(t)\}$:

$$s_k = \sum_{n=0}^{2N-1+\mu} w[n] e^{j(2\pi n f/f_s)} \int_{-\infty}^{\infty} S(f) e^{-j(\pi n/N)k} df \quad (5)$$

$$= \int_{-\infty}^{\infty} S(f) \sum_{n=0}^{2N-1+\mu} w[n] e^{j(2\pi n f/f_s) - j(\pi n/N)k} df \quad (6)$$

$$= \int_{-\infty}^{\infty} S(f) G_k(f) df \quad (7)$$

where we interpret $G_k(f)$ as a *transfer function* (Dirichlet kernel [15]) from the unknown RF signal's Fourier transform $S(f)$ to its DFT coefficients s_k. We parameterize $G_k(f)$ in Appendix B by means of a Taylor expansion. This leads to the following linear model of the RFI:

$$\widetilde{s}_k = \sum_{l=0}^{L-1} c_l G_k^{(l)}(+\widehat{f}_c) + \sum_{m=0}^{M-1} (-1)^m c_m^* G_k^{(m)}(-\widehat{f}_c) \quad (8)$$

where $\widehat{f}_c$ is an estimate of the center frequency, $G_k^{(l)}\left(+\widehat{f}_c\right)$ is the lth derivative of $G_k(f)$ at $\widehat{f}_c$, and $\{c_l\}$ *are unknown parameters* modeling the RFI. This can be written in a matrix notation as

$$\mathbf{s} \approx \widetilde{\mathbf{s}} \triangleq \mathbf{G}\mathbf{c} \quad (9)$$

where $\mathbf{G}$ is derived from $G_k(f)$ (10) as shown at the bottom of the page, and $\mathbf{c}$ is the vector containing unknown RFI parameters

$$\mathbf{c} = (\, c_0 \quad \dots \quad c_{L-1} \quad c_0^* \quad \dots \quad (-1)^{M-1} c_{M-1}^* \,)^T. \quad (11)$$

The conjugated parameters in (11), which corresponds to contributions from negative frequencies, gives almost no contribution to $\widetilde{\mathbf{s}}$ when windowing is used as in Appendix A and Section VI. Then, the sizes of the vector $\mathbf{c}$ and the matrix $\mathbf{G}$ can be reduced

$$\mathbf{G}_{\text{wind}} = \begin{pmatrix} G_0(\widehat{f}_c) & \cdots & G_0^{(L-1)}(\widehat{f}_c) \\ \vdots & \vdots & \vdots \\ G_{N-1}(\widehat{f}_c) & \cdots & G_{N-1}^{(L-1)}(\widehat{f}_c) \end{pmatrix} \quad (12)$$

$$\mathbf{c}_{\text{wind}} = (\, c_0 \quad \dots \quad c_{L-1} \,)^T, \quad (13)$$

with a negligible performance loss. This will be applied in Section VI.

B. Disturbance Estimation and Cancellation

In the matrix formulation, our model for the received signal on *unused* (silent) tones becomes

$$\mathbf{r}_{\mathcal{U}} = \widetilde{\mathbf{s}}_{\mathcal{U}} + \mathbf{n}_{\mathcal{U}} = \mathbf{G}_{\mathcal{U}}\mathbf{c} + \mathbf{n}_{\mathcal{U}} \quad (14)$$

where $\mathcal{U} = \{k_1, k_2, \dots, k_{|\mathcal{U}|}\}$ denotes the index set for the tones on which we measure the RF disturbance. Assuming that the noise $\mathbf{n}_{\mathcal{U}}$ is independent and identically Gaussian distributed, we obtain an maximum likelihood estimate, $\widehat{\mathbf{c}}_{ML}$, of the parameters $\mathbf{c}$ when windowing is used [16]

$$\widehat{\mathbf{c}}_{ML} = \mathbf{G}_{\mathcal{U}}^{\dagger}\mathbf{r}_{\mathcal{U}} \quad (15)$$

where $\mathbf{G}_{\mathcal{U}}^{\dagger}$ is the pseudoinverse of $\mathbf{G}_{\mathcal{U}}$. We have then assumed that $\mathbf{G}_{\mathcal{U}}$ has full column rank. If windowing is not used (i.e., also the negative frequencies will contribute), we need to rewrite $\mathbf{G}_{\mathcal{U}}$, $\mathbf{c}$ and $\mathbf{r}_{\mathcal{U}}$ slightly to separate the real and imaginary parts before the pseudoinverse is calculated since the coefficient vector $\mathbf{c}$ contains both the parameters c_l and the complex conjugates c_l^*.

Now, let the index set $\mathcal{M}$ indicate the modulated DMT tones. By using $\widehat{\mathbf{c}}_{ML}$, we obtain the estimates of the disturbance as

$$\widehat{\mathbf{s}}_{\mathcal{M}} = \mathbf{G}_{\mathcal{M}}\widehat{\mathbf{c}}_{ML} = \mathbf{G}_{\mathcal{M}}\mathbf{G}_{\mathcal{U}}^{\dagger}\mathbf{r}_{\mathcal{U}} = \widetilde{\mathbf{s}}_{\mathcal{M}} + \mathbf{G}_{\mathcal{M}}\mathbf{G}_{\mathcal{U}}^{\dagger}\mathbf{n}_{\mathcal{U}}. \quad (16)$$

Finally, we use these estimates to reduce the effect of the disturber by subtracting them from the data

$$r_k - \widehat{s}_k = x_k h_k + (s_k - \widehat{s}_k) + n_k. \quad (17)$$

IV. Frequency Invariance

Frequency invariance is an interesting complexity reducing property that follows from the construction of the canceller and due to the properties of the DFT. It means that the same precalculated estimator coefficients, given by the matrix $\mathbf{G}_{\mathcal{M}}\mathbf{G}_{\mathcal{U}}^{\dagger}$ in (16), can be used by the canceller practically independent of the RFI signal's frequency location[1]. As a consequence, no recomputation (or initialization) of the canceller is needed if a frequency shift of the RFI signal occurs, e.g., if a radio amateur suddenly change its transmission frequency to a different HAM band.

This property is also valuable for cancelling several frequency separated RFIs; they can all be cancelled using the same estimator coefficients. The theoretical and practical requirements for the frequency invariance property are similar to [17] and explored for this canceller in detail below.

The set of theoretical conditions required for maintaining the same estimator coefficients for the RFI canceller are

1) The RFI signal's frequency shift is an integer number of subcarriers $f_{c_1} = f_{c_0} + (k_1/2N)f_s$, $k_1 \in Z$, where f_{c_1} and f_{c_0} represent the new- and previous RFI center frequencies, respectively.

   Remark: In practice, with a robust canceller design noninteger frequency shifts can also be handled. The robust-

[1]The only exceptions are if the RFI signal would be located either very close to the dc level or the Nyquist frequency, i.e., the lowest or highest subcarriers.

$$\mathbf{G} = \begin{pmatrix} G_0(\widehat{f}_c) & \dots & G_0^{(L-1)}(\widehat{f}_c) & G_0(-\widehat{f}_c) & \dots & G_0^{(M-1)}(-\widehat{f}_c) \\ \vdots & \vdots & \vdots & \vdots & \vdots & \vdots \\ G_{N-1}(\widehat{f}_c) & \dots & G_{N-1}^{(L-1)}(\widehat{f}_c) & G_{N-1}(-\widehat{f}_c) & \dots & G_{N-1}^{(M-1)}(-\widehat{f}_c) \end{pmatrix} \quad (10)$$

ness of the canceller is related to the number of model parameters selected which is a designers choice.

2) Sufficient nonrectangular receiver windowing is applied so that RFI spectral leakage from the negative frequency component of the RFI can be neglected. That is, G_{wind} in (12) is used.

   Remark: If no windowing is used, some complexity savings can still be achieved, see below.

3) The measurement tones are circular shifted accordingly to around the new frequency position, f_{c_1}. That is, $\mathcal{U}_1 = \{(k+k_1) \bmod 2N | \, k \in \mathcal{U}_0\}$, where $\mathcal{U}_1$ and $\mathcal{U}_0$ are the new and old sets of measurement tone indexes, respectively, and mod represents the modulo operator.

When a frequency shift of the RFI occurs, the Dirichlet kernel function $G_k(f)$ (26) can be expressed as

$$G_k(f_{c_1}) = \sum_{n=0}^{2N-1+\mu} w[n] \times e^{j(2\pi n f_{c_1}/f_s) - j(\pi n/N)k}\Big|_{f_{c_1}=f_{c_0}+(k_1/2N)f_s} \tag{18}$$

$$= \sum_{n=0}^{2N-1+\mu} w[n] e^{j(2\pi n f_{c_0}/f_s) - j(\pi n/N)(k-k_1)} = G_{k-k_1}(f_{c_0}). \tag{19}$$

Hence, when $M = 0$ (that is, with windowing applied) the matrix $\mathbf{G}_{\mathcal{M}_1}$ after the frequency shift is similar to $\mathbf{G}_{\mathcal{M}_0}$ before the shift, just with its rows circularly shifted

$$\mathbf{G}_{\mathcal{M}_1(l,m)} = \mathbf{G}_{\mathcal{M}_0((l+k_1) \bmod 2N, m)}. \tag{20}$$

With a replacement of the measurement tones according to requirement 3 above $\mathbf{G}_{\mathcal{U}} = \mathbf{G}_{\mathcal{U}_0} = \mathbf{G}_{\mathcal{U}_1}$ and thus also $\mathbf{G}^{\dagger}_{\mathcal{U}}$ remain the same. The end result is then only that the final estimator coefficients just becomes circularly shifted in the rows

$$\begin{aligned} \mathbf{G}^1 &\triangleq \mathbf{G}_{\mathcal{M}_1}\mathbf{G}^{\dagger}_{\mathcal{U}} \\ &= \mathbf{G}_{\mathcal{M}_0((l+k_1) \bmod 2N, m)}\mathbf{G}^{\dagger}_{\mathcal{U}} \\ &= \mathbf{G}^0_{((l+k_1) \bmod 2N, m)}. \end{aligned} \tag{21}$$

Alternatively, one can use the old estimator coefficients $\mathbf{G}^0 = \mathbf{G}_{\mathcal{M}_0(l,m)}\mathbf{G}^{\dagger}_{\mathcal{U}}$ and instead circularly shift the estimated vector before it is cancelled from the tones

$$\widehat{\mathbf{s}}_{\mathcal{M}_1((l+k_1) \bmod 2N)} = \widehat{\mathbf{s}}_{\mathcal{M}_0(l)}. \tag{22}$$

If no windowing is applied, however, some parameters ($M > 0$) that models spectral leakage from the negative frequency peak should be included in the canceller. In this case, the $\mathbf{G}$ matrix's (10) L first columns (and therefore also $\mathbf{G}_{\mathcal{M}_1}$) need to be circularly shifted in the rows as described above and the last M columns need to be circularly shifted in the rows but in the opposite direction with the same amount, k_1. Again, this means that all its elements can be reused but $\mathbf{G}_{\mathcal{U}_1}$ has new elements from the doubly shifted $\mathbf{G}$ which requires new computations of $\mathbf{G}^{\dagger}_{\mathcal{U}_1}$ and the matrix product $\mathbf{G}_{\mathcal{M}_1}\mathbf{G}^{\dagger}_{\mathcal{U}_1}$.

V. Complexity

The complexity of the algorithm is best evaluated in two parts; offline initialization and running cancellation during online operation. Below we make a sketch of the number of multiplications that are required for each part.

A re-initialization is usually required when the characteristics of the RFI signal drastically changes, i.e., when the design parameters must be changed. An example is that for a cancellation of AM radio RFI with a up to 10-kHz bandwidth instead of HAM radio with up to 4-kHz bandwidth, more model parameters should be included into the canceller to be able to suppress the wider AM radio signal bandwidth.

However, note that due to the frequency invariance of the canceller a RFI frequency change, e.g., to a different HAM band, the canceller needs not be updated. But, when two or more RFIs are located quite closely and spectral leakage occurs from one peak to another a re-initialization needs to be done using a resembling RFI signal model. The need of re-initialization in this case depends also on the amount of windowing used which suppresses the leakage between different RFI peaks.

Note, however, that in the case of several RFIs it is most likely that they are somewhat separated in frequency. Two or more very close RFIs are unlikely simply because they would then interfere with each other. In practise, a set of estimator coefficients representing the most likely scenarios, e.g., AM and HAM radio, can be precalculated off-line and stored in each modem—ready to be swapped during on-line operation.

A. Initial Complexity

The initial complexity consists of computing the matrices $\mathbf{G}_{\mathcal{M}}$ and $\mathbf{G}^{\dagger}_{\mathcal{U}}$ in (16) for a new scenario prior the running, frame-by-frame, cancellation. $\mathbf{G}_{\mathcal{M}}$ and $\mathbf{G}_{\mathcal{U}}$ can be obtained from the full $\mathbf{G}$ matrix (10) which requires $(L+M)$ DFTs each of length $2N$, thus $2N(L+M)\log(2N)$ multiplications. Note, however, to increase the supported cancellation bandwidth, e.g., by increasing L by one, only one extra $2N$-DFT need to be computed for the full $\mathbf{G}$ matrix.

The calculation of the pseudo-inverse, $\mathbf{G}^{\dagger}_{\mathcal{U}}$, requires $O(|\mathcal{U}|^3)$ multiplications. In total, the initialization is of $O(2N)+O(|\mathcal{U}|^3)$ multiplications, which is typically dominated by the first term. In the performance evaluation below, $L = 0$, $M = |\mathcal{U}| = 2$, $N = 256$ or 2048.

B. Runtime Complexity

Once the estimator coefficients are derived, the runtime complexity consists mainly of the multiplication $\mathbf{G}_{\mathcal{M}}\widehat{\mathbf{c}}_{ML}$ in (16). This takes $|\mathcal{M}|\,|\mathcal{U}|$ complex multiplications per DMT frame, where $|\mathcal{M}| < N$, is the number of tones with RFI cancellation. That is, less than $|\mathcal{U}|/2$ complex multiplications per sample are required. When nonrectangular windowing is performed, it takes 2μ additional multiplications per DMT frame which corresponds to fewer than μ/N multiplications per sample. The actual estimation of $\widehat{\mathbf{c}}_{ML}$ requires only $|\mathcal{U}|^2$ multiplications per DMT frame, or less than $|\mathcal{U}|^2/2N$ per sample.

TABLE II
SIMULATION PARAMETERS

AWGN level	-140 dBm/Hz
Sampling frequency	$f_s = 22$ MHz
RF center frequency	$f_c = 3.79$ MHz
Wire length	1000 m
Cable type	TP1
Number of DMT-tones	$N = 256/2048$
Window length	$\mu = 20/70$

VI. PERFORMANCE EVALUATION

We illustrate our digital RFI cancellation method on two example systems: one with 256 DMT tones and one with 2048 tones. The environment is fixed to a 1000-m long TP1 cable [18] where the noise consists of 49 self-FEXT disturbers plus AWGN with a spectral density of – 140 dBm/Hz. The sampling frequency is $f_s = 22$ MHz. Table II summarizes the simulation parameters. We let the RFI signal have the same average power as the desired signal after demodulation. The RFI signal has a SSB–SC modulation where the baseband envelope ($b(t)$ in (24)) is constructed by filtering complex white noise through a third order Butterworth filter, with parameters selected to match the specific RFI bandwidth under study. Hence, the power-spectral density (PSD) of the RFI is $B(f - f_c) + B^*(-f - f_c)$ where $B(f)$ is a third order Butterworth spectrum. We measure the performance in terms of RFI suppression and average SNR-loss due to the remaining RFI disturbance. The SNR-loss is averaged over all DMT tones that are used for transmission. Without the RFI disturbance, the average SNR is 24 dB in these scenarios.

Throughout the evaluation, we use two parameters to model the RFI and also two measurement tones. Two parameters is a good tradeoff since one parameter does not give satisfactory performance and the improvement by adding a third parameter (and the corresponding complexity) is small. The reason for this is related to the time–bandwidth product of the RFI signal and the inter tone spacing of the DMT–VDSL system, see [17]. Furthermore, since we allow a narrow residual RFI peak between the measurement tones, and windowing is used, fewer model parameters are needed than the actual time–bandwidth product specifies which motivates why only two parameters suffice.

In practice, it may be sound to measure on more tones than the number model parameters used to increase the method's robustness against noise. In our simulations, however, using more tones does not give any large improvement. Which tones to measure on is dependent on the total number of DMT tones in the system, the width of the HAM band and the number of tones to be used. The choice of measurement tones should be done with care since it has an impact on performance, as we will see later on.

We examine the cases with and without windowing in the system. When windowing is performed, we use $\mu = 20$ extra samples $(N = 256)$ in the cyclic extension as described in Appendix B, and when $N = 2048$ we use $\mu = 70$ extra samples for windowing. In all simulations the center frequency of the RF signal is located just at the edge of the second HAM band, $f_c = 3.79$ MHz, (adjusted a few kilohertz to put it exactly between two DMT tones where it makes the most damage to a DMT system). However, the RFI cancellation method works just as well in all HAM bands.

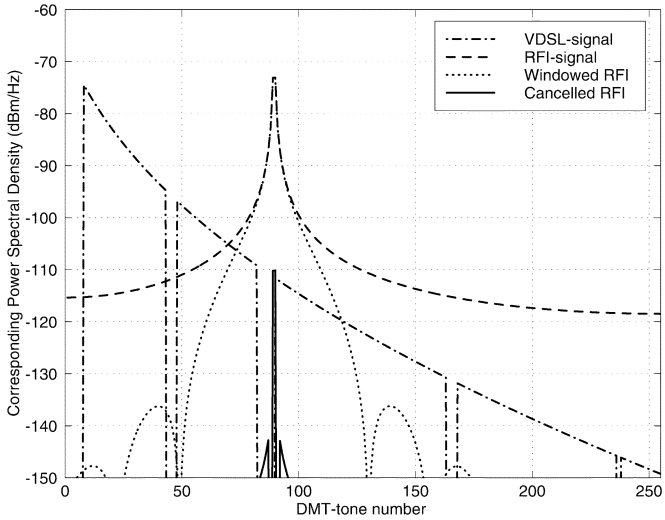

Fig. 3. Corresponding PSD of RFI signal before and after RFI cancellation for 256 DMT tones.

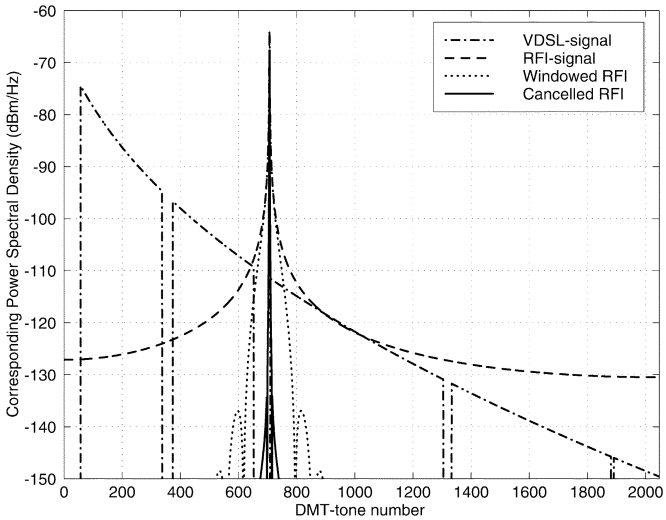

Fig. 4. Corresponding PSD of RFI signal before and after RFI cancellation for 2048 DMT tones.

As a starting example, we examine the PSD of the RFI before and after windowing and RFI cancellation, for a typical case. The RF signal has 5-kHz bandwidth and the center frequency is assumed to be known. Figs. 3 and 4 show the corresponding PSDs[2] for this case. We can see that the windowing alone suppresses the RFI on many tones, implying that fewer tones need RFI cancellation, but those closest to the center frequency still get a considerable amount of RFI. We also find that with cancellation the RFI is almost completely removed. The gaps in the RFI cancelled curves, which are present in all PSD figures throughout the paper, represent the locations of the measurement tones and cannot be used for data transmission. Only a few tones located near the RFIs center frequency, between the measurement tones within the HAM band, have strong residual RFI.

Because of the RFI suppression by the window, the interference contribution from negative frequencies can be neglected in

[2]The spectral "power" of all signals in the DMT domain is scaled to the corresponding PSD levels of the physical, time continuous, signals.

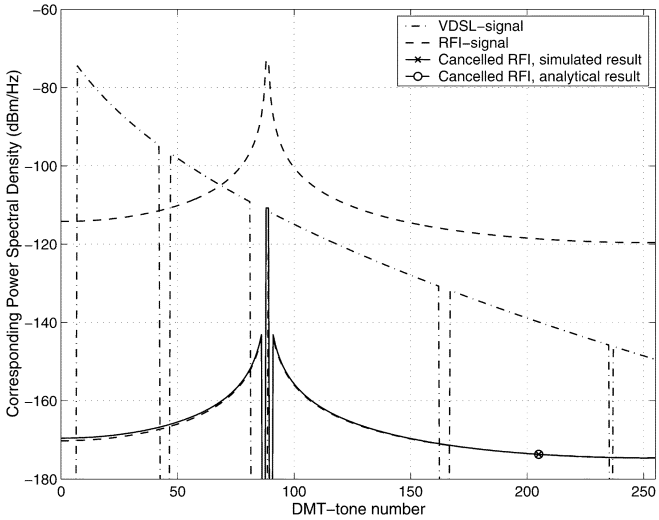

Fig. 5. Simulated and analytical results of cancelling a 5-kHz wide RFI, 256 tones.

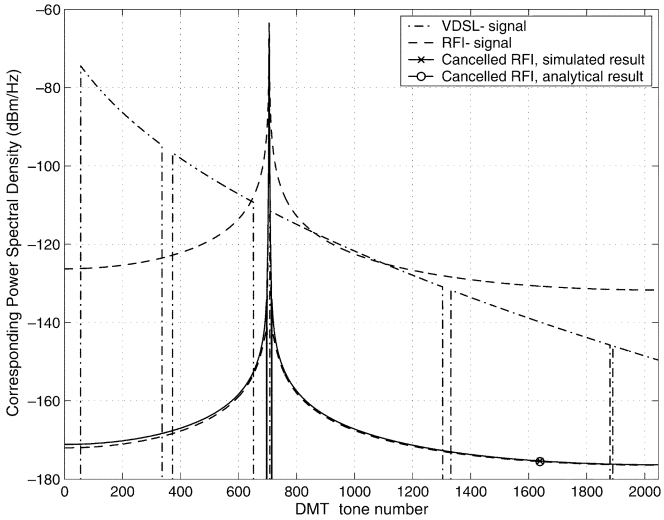

Fig. 6. Simulated and analytical results of cancelling a 5-kHz wide RFI, 2048 tones.

the RFI cancellation, allowing the reduced (12) and (13) to be used. Since windowing also reduces the number of tones that need RFI cancellation, the complexity of the RFI canceller is reduced. Another advantage is that if, in an unlikely situation, there would be more than one RFI signal (in different HAM bands) then they can be cancelled independently. Windowing gives better performance for systems with more DMT tones (measured in the number of samples), because a larger window can be used with the same efficiency loss.

A. Analytical Comparisons to Monte Carlo Simulations

The performance evaluation herein is based on Monte Carlo simulations in which we simulate narrow-band RFI cancellation. We construct the baseband parts of the simulated RFI signals ($b(t)$ in (24)) using a third order Butterworth filter, with parameters selected to match the specific RFI bandwidth under study. However, it is possible to validate the results from simulations by performing an analytic (fully theoretic) comparison using the methods described in [17]. For this comparison, it is necessary to select some appropriate PSD that analytically models the simulated RFI spectrum well, in order to get a good agreement between analytical and simulated results.

Fig. 5 shows, for 256 DMT tones, the result of cancelling a 5-kHz wide RFI using MC simulations and the corresponding analytical PSD resulting from cancelling an RFI signal with a Gaussian PSD shape. The 5-kHz cutoff frequency in the analytical Gaussian PSD model was set at − 4 dB to closely match the simulated results. Fig. 6 shows corresponding simulated and analytical results for 2048 tones. In order to emphasize the differences between analytical and simulated results in these comparisons, no receiver windowing was applied before the cancellation. Clearly, using receiver windowing ($\mu > 0$) does not change this good agreement.

B. Increasing Bandwidth of the RFI

In this simulation, we assume that the center frequency of the RFI signal is known, i.e., $\widehat{f}_c - f_c = 0$, and we let the bandwidth of the RF signal increase from 0 to 20 kHz ($f_c = 3.79$ MHz).

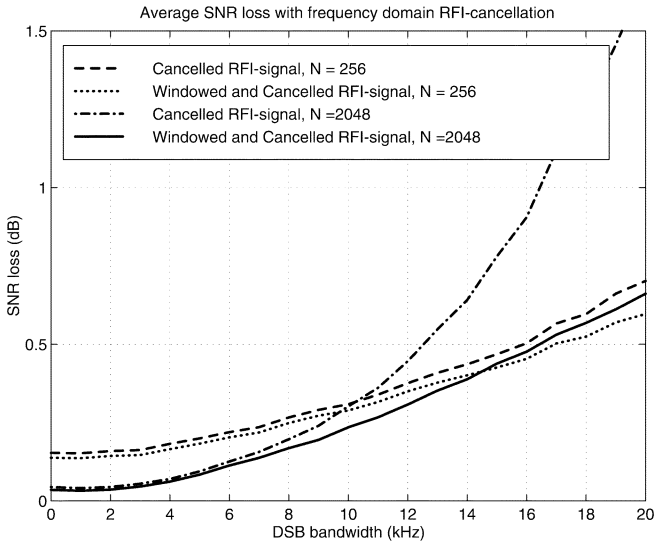

Fig. 7. SNR loss after RFI cancellation and with/without windowing in the receiver.

Normally the bandwidth of an amateur radio signal is in the order of 3 kHz. We are using two parameters to model the RFI and also two measurement tones. For $N = 256$ we use the two tones with indexes {#87,#90} which are one tone away from the tones with the most RFI {#88,#89}. When $N = 2048$ we use the measurement tones {#697,#714}, which are eight tones away from the tones with the most RFI {#705,#706}.

Fig. 7 shows the average SNR loss after the RFI cancellation and windowing. The method performs very well for both 256 and 2048 DMT tones, both with and without the use of a window in the receiver, although windowing prior to cancellation yields a little bit better performance. If the bandwidth of the RFI is smaller than 10 kHz the average SNR loss is reduced to less than 0.3 dB with the RFI canceller in all cases.

Figs. 8 and 9 show the PSD of the RFI before and after RFI cancellation. The gaps in the plots indicate where the measurement tones are located. The RFI level on the left hand side of Figs. 8 and 9, where the RFI is strong, is inside the HAM band.

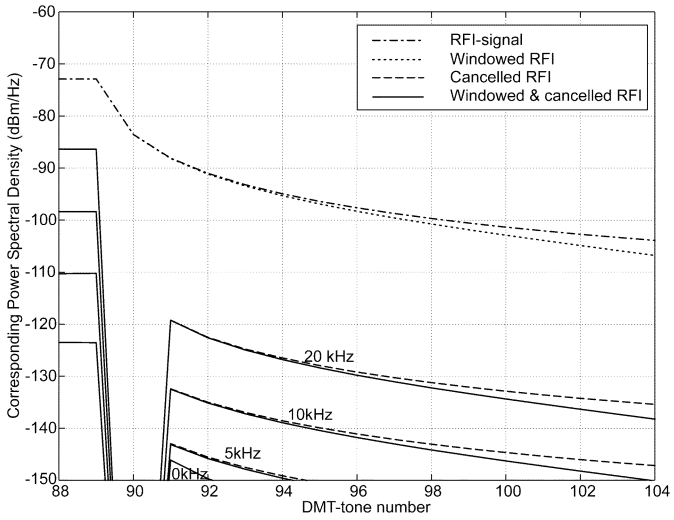

Fig. 8. Corresponding PSD of RFI signal with varying bandwidth, before and after RFI cancellation for 256 DMT tones. The signal left part of the figure is inside the HAM band. (Compare with Fig. 3 which has a different scale).

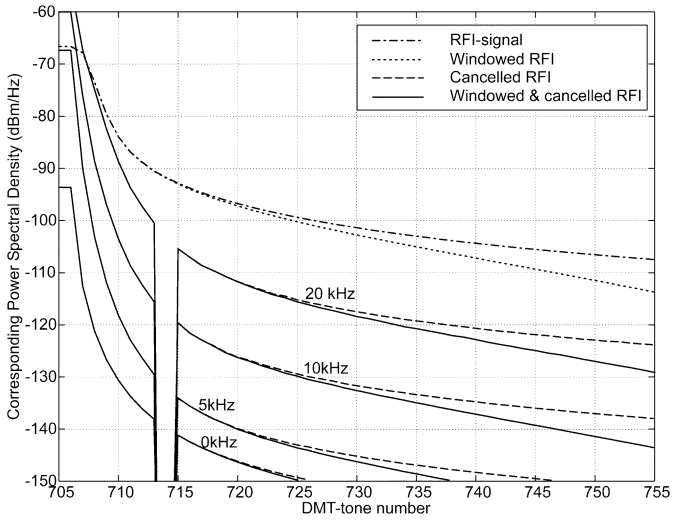

Fig. 9. Corresponding PSD of RFI signal with varying bandwidth, before and after RFI cancellation for 2048 DMT tones. The signal left part of the figure is inside the HAM band. (Compare with Fig. 4 which has a different scale).

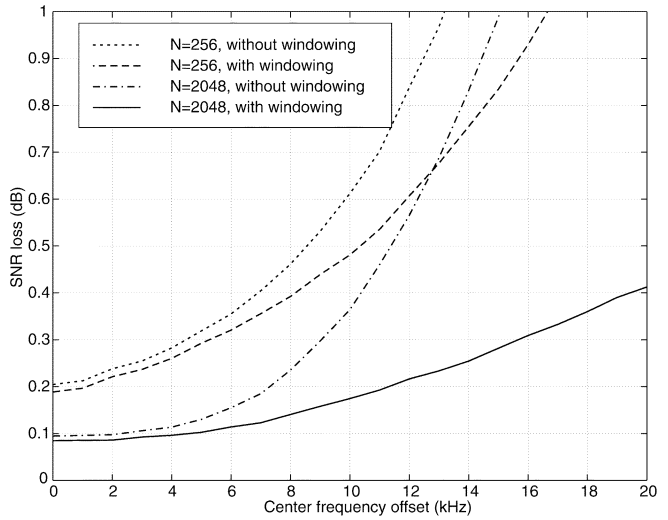

Fig. 10. Average SNR loss after RFI cancellation, with/without windowing in the receiver, when the center-frequency estimation error goes 0–20 kHz.

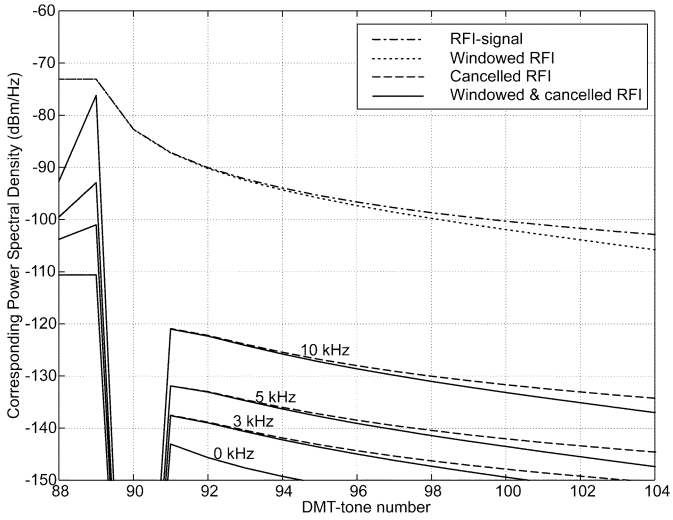

Fig. 11. Corresponding PSD of RFI signal with different frequency offsets, before and after RFI cancellation for 256 DMT tones.

Note the similarity with Figs. 3 and 4, but with a much different scale on the horizontal axis.

Considering RF signals with at most 5-kHz bandwidth, we find that just a few tones away from the center of the RFI the RFI suppression is 40–50 dB and the residual RFI is below the AWGN noise floor at -140 dBm/Hz. For 256 DMT tones the noise floor is reached within only two tones, for 2048 DMT tones the noise floor is reached after about 16 tones. Thus, the relative number of tones that is affected by residual RFI is approximately the same in both cases.

C. Impact of Frequency Estimation Errors

When deriving the RFI canceller, the center frequency of the RFI must be known. However, in practice, we never know the center frequency exactly, it has to be estimated in some way. In this subsection we look at how the performance of the RFI canceller depends on the accuracy of the center frequency estimates. We fix the bandwidth of the RF signal to 5 kHz and let the error in the center-frequency estimate, $\widehat{f}_c - f_c$, vary between 0 and 20 kHz. The same measurement tones as in the previous simulation are used. Fig. 10 shows performance in terms of average SNR-loss, and Figs. 11 and 12 show the RFI in the DFT-domain.

For frequency errors up to 5 kHz, the canceller suppresses the RFI about 35–40 dB (except for a few tones near the center of the RFI), so only a coarse estimate of the center frequency is required. By searching for the tone with the most RFI, we get an estimate of the center frequency with at least half the tone-spacing accuracy. When 2048 tones are used, the tone-spacing is 5.4 kHz. Thus the error in the center-frequency estimate becomes at most 2.7 kHz. When fewer tones are used some other method must be used for frequency estimation. A simple and robust method is derived in [11] (see also [12]) and works as follows. Let the interferer be located at frequency

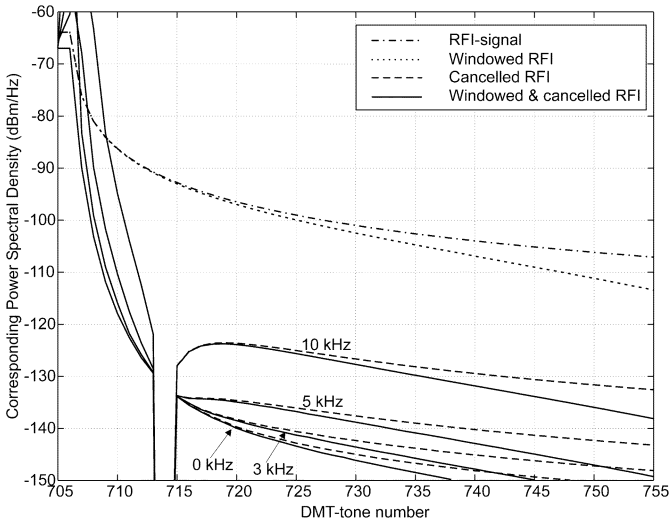

Fig. 12. Corresponding PSD of RFI signal with different frequency offsets, before and after RFI cancellation for 2048 DMT tones.

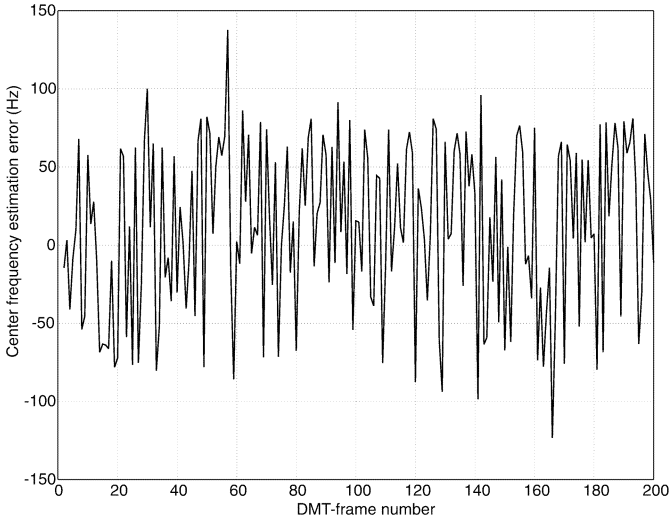

Fig. 13. Center frequency estimation error for 200 DMT frames with 256 tones.

$f_c = (k_0 + \delta)(f_s/2N)$ where $0 \leq \delta < 1$ is the offset from a DMT tone at frequency $k_0(f_s/2N)$. The tone-index k_0 can easily be found by searching for the two tones $(k_0, k_0 + 1)$ that has most RFI. Then the offset can be well approximated with

$$\delta \approx \frac{|r_{k_0+1}|}{|r_{k_0}| + |r_{k_0+1}|} \tag{23}$$

where r_{k_0} is the received signal on tone k_0. Fig. 13 shows the performance of this estimator for a simulation of 200 DMT frames with 256 tones. In this case, the estimation error was always smaller than 150 Hz, which is very small considering that we can tolerate errors up to several kilohertz.

D. Placement of Measurement Tones

So far, we have used the same set of measurement tones when estimating the RFI parameters. In this last simulation we examine how the choice of measurement tones affects the performance of the canceller, still using only two model parameters and two measurement tones on each side of the center frequency of the RFI. Once again, the RFI is fixed at 3.79 MHz with a 5-kHz bandwidth and the center frequency is assumed to be known. Fig. 14 shows the performance in terms of average SNR-loss. Using the two tones with the most RFI corresponds to 0 on the x-axis in the figure. Figs. 15 and 16 show the remaining RFI in the DFT domain.

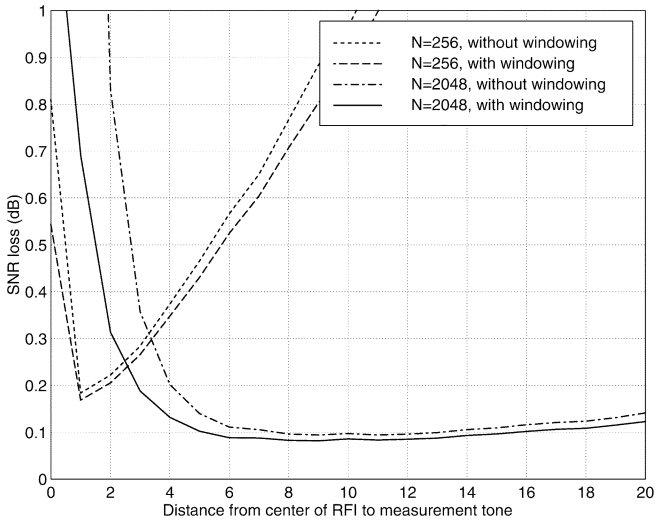

Fig. 14. Average SNR loss for different choices of measurement tones. $N = 256/2048$, $\mu = 20/70$, and RFI bandwidth = 5 kHz.

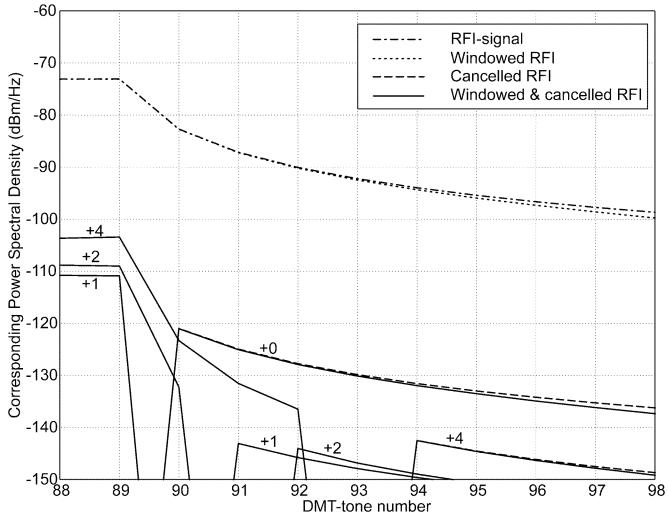

Fig. 15. Corresponding PSD of RFI signal before and after RFI cancellation for 256 DMT tones and with different distances $(+0, +1, +2, +4)$ between the measurement tones and the center of the RFI. (The gaps appear where the measurement tone is placed).

As the figures show, one should avoid to use the tones closest to the RFI as measurement tones, especially when many subcarriers are used. For 256 tones the best performance is achieved when the measurement tones are the two next to the two tones with most RFI (distance ± 1 subcarriers from the RFI center). When 2048 tones is used the measurement tones should be placed 8–14 tones away from the center of the RFI to give the best result.

In the performance evaluations in this paper, the model error depends essentially on the few model parameters selected in order to keep complexity at a low level. The RFI signal's order

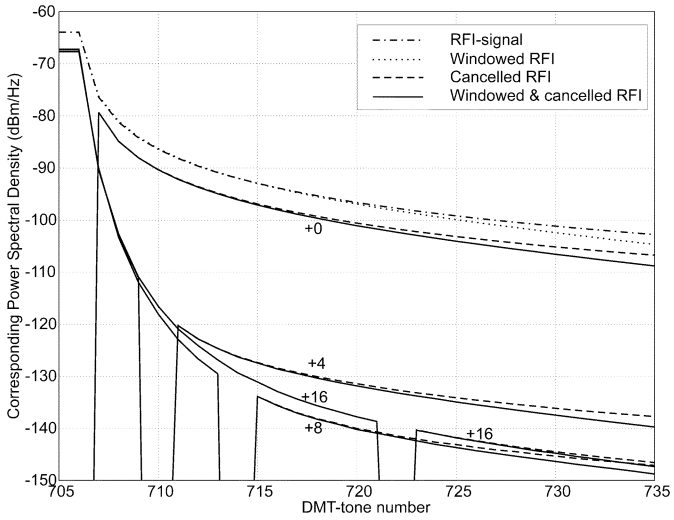

Fig. 16. Corresponding PSD of RFI signal before and after RFI cancellation for 2048 DMT tones and with different distances $(+0, +4, +8, +16)$ between the measurement tones and the center of the RFI. (The gaps appear where the measurement tone is placed).

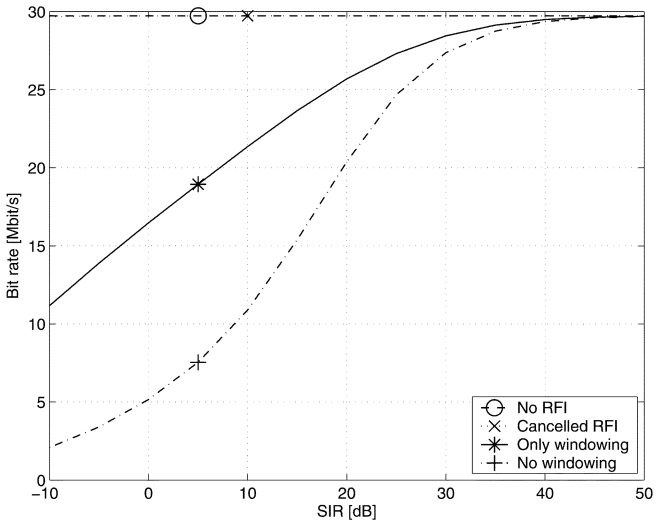

Fig. 17. Bit rates with/without RFI, windowing, and RFI cancellation as a function of SIR. A typical practical working point could be 0-dB SIR, on the basis that an analog RFI canceller should suppress RFI to this level in order to protect the ADC from clipping.

is highest (most concentrated) at subcarriers close to the peak and lower on subcarriers away from it where the RFI spectral leakage occurs. It is those tones further away that need RFI suppression since they are used for data transmission. Hence, with a lower model order than the actual RFI signal the RFI spectral leakage can be suppressed effectively but not the RFI peak itself. However, the interference at the peak is of little interest since it has no effect on the DSL performance.

For the reasons explained, the best placement of the measurement tones is a tradeoff between low model error and high signal-to-noise ratio (RFI/noise). When the measurement tones are placed very close to the RFI peak the model error will degrade the estimates of the coefficients more, $\widehat{\mathbf{c}}_{ML}$ in (15), but the SNR is very good. When the measurement tones are placed further away from the RFI peak the effects of model errors are reduced but the SNR is also lower. Note, however, that with a larger model order than selected here (and more measurement tones) the peak can also be effectively suppressed but in this case the measurement tones should instead be placed on and around the RFI peak [17].

E. Bit- and Symbol-Error Rate Evaluation

In the previous evaluations, we examined specifically the SNRs or PSDs before and after RFI cancellation. In this section, we also exemplify the bit-rate and symbol-error rate performances with and without RFI cancellation and receiver windowing to further emphasize the necessity of cancellation in the presence of RFI. Note, however, that for the case with no RFI cancellation, our bit-rate evaluation assumes that the RFI is stationary on a given frequency location so that training, initialization and proper bitloading according to the present RFI can be achieved. On the contrary, HAM amateur radio has typically a quite nonstationary behavior. Radio amateurs frequently change their transmission frequency within the HAM bands. Additionally, the transmission activity (with Morse code, data, or voice using single duplex) has short, but frequent, silent periods. Hence, without RFI cancellation this would cause frequent error bursts (or require the use of extensive channel coding and interleaving) and the need of frequent re-initializations for updating the bitloading due to the varying noise environment. With RFI cancellation, however, the bitloading can remain constant without causing error bursts since the RFI can be effectively suppressed below the dominating background noise (the FEXT on most subcarriers) even when the frequency location of the RFI changes, thereby avoiding frequent re-initializations.

Fig. 17 shows examples of the bit-rates for varying *signal-to-interference ratios* (SIRs). In this evaluation it is assumed that the bitloading is proper, that is, yielding less than 10^{-7} symbol-error rate (SER) in each case. The RF signal bandwidth is 5 kHz and the RFI is located in the first HAM band. With RFI cancellation, the bit-rates are nearly identical to when no RFI is present and they are significantly improved compared to when no RFI cancellation is performed.

The practical bit rate can vary depending on a number of other factors like RFI frequency position, cable type and length, level of other background noise (crosstalk), length and type of nonrectangular window, number of subcarriers, etc. Nevertheless, this example illustrates the characteristic and relative performance with/without RFI cancellation and nonrectangular receiver windowing.

Fig. 18 shows the corresponding SERs for the case when the bitloading is performed without any RFI present, that is, it matches the bit rate with no RFI which is 29.7 Mb/s as in Fig. 17. These error rates are obtained by first computing the average SNR on each tone from 10^5 simulated DMT frames, with and without RFI cancellation. Then, the SER values are found by using the analytic[3] formulae for M-QAM constellations and by assuming that the noise (residual RFI, FEXT and AWGN) is Gaussian distributed on each subcarrier. In this mismatched bitloading scenario, the effect of windowing is minor

[3]Due to the low target SER for DSL, accurate values through simulations are difficult to obtain.

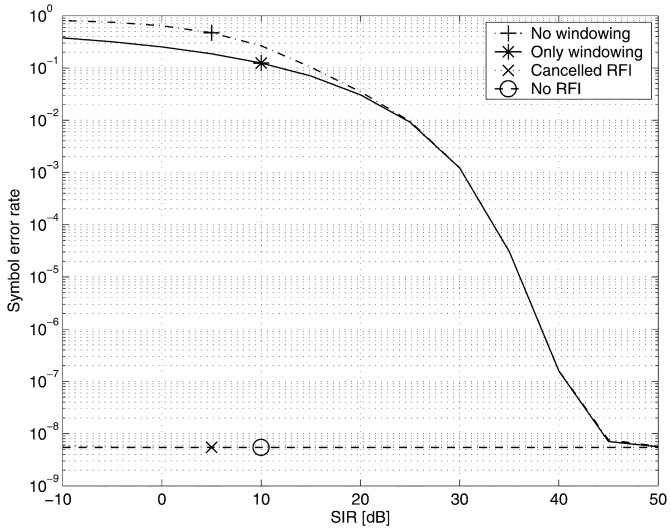

Fig. 18. SERs when the bitloading is performed without any RFI present.

and symbol errors become common also for relatively high SIR if no cancellation is performed. These errors are most common on subcarriers close to the RFI center frequency, where windowing (independent of type) has almost no suppression effect as shown in previous PSD plots. With cancellation, however, an increased SER can be avoided.

VII. Summary

We have derived a frequency-domain RFI cancellation method for DMT-based VDSL-systems. The only assumptions made about the RF signal are that it is narrow-band and that its center frequency is approximately known or estimated, which we also describe how to estimate.

By measuring the disturbance on a number of unused (silent) DMT tones in the HAM bands we are able to subtract estimates of the RFI from the modulated DMT tones. Some of the main characteristics of the resulting method are as follows.

- It works for practically any number of DMT tones, e.g., 256 and 2048.
- It works both for systems with nonrectangular receiver window and for systems with rectangular window (no windowing).
- It is quite insensitive to errors in the estimate of the center-frequency. For DMT system with many tones, e.g., 2048, it is sufficient to know between which tones the RFI is located, but for systems with fewer tones a simple frequency estimation routine is required.
- The performance is almost the same with and without windowing. Windowing, however, allows reducing the complexity of the RFI canceller as fewer tones need to be corrected by the RFI canceller. If 2048 tones is used, only about 200 of them need to be corrected.
- Using windowing gives a simpler RFI canceller since the contribution from negative frequencies can be neglected, and several RFI disturbances can be cancelled individually.

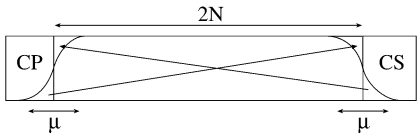

Fig. 19. Windowing the DMT frame by "cut and paste."

- The method almost completely cancels the RFI from nearly all used DMT tones, leaving only a few tones affected by residual RFI. The average RFI suppression is 40–50 dB and the resulting average SNR-loss is reduced to less than 0.3 dB for RF bandwidths up to 5 kHz.

Appendix A
Windowing the DMT Frame

Windowing the received DMT frame can be performed to improve the RFI rejection, among other things. The reception of RFI from a narrow-band RF signal will extend out on all carriers due to the strong sidelobes from a rectangular window on the DMT frame. A nonrectangular window can reduce the reception of RFI on the DMT carriers due to suppression of the sidelobes. In order to maintain orthogonality between the tones, the receive window needs to be extended beyond the $2N$-sample boundary of the DMT symbol but still within the cyclic extension. We use a window with pulse-shaped wings that have a raised cosine form (one possible choice) of length μ as sketched in Fig. 19. By moving the $\mu/2$ samples long tails of the window [7] and adding them to their respective reverse side of the DMT symbol, as shown in Fig. 19, the original $2N$ size FFT need not to be increased. Due to the periodicity of the DMT symbol and the symmetry of the window this procedure will act as a folding of the windowed DMT symbol. The folding results from decimating the $2N + \mu$ long symbol in the frequency domain down to $2N$ samples.

Appendix B
Parameterization of RFI

We will derive the method using two different approaches: one frequency-domain and one time-domain. The frequency-domain derivation contains an ad-hoc Taylor expansion in the frequency domain, the time-domain method uses an ad-hoc signal model. However, we will find that they both result in same RFI canceller.

Proceeding with the model of the RF signal $s(t)$, we write it as

$$s(t) = b(t)e^{i2\pi f_c t} + b^*(t)e^{-i2\pi f_c t} \tag{24}$$

where $b(t)$ is the narrow-band baseband equivalent of the RF signal, and the asterisk denotes complex conjugate. This choice of model is based on that the RF signal is narrow-band, typically in the order of a few kilohertz of bandwidth, and it can represent any type of analog modulation, amplitude modulation, double sideband modulation (DSB), single sideband modulation, etc.

A. Frequency-Domain Approach

We assume that the disturbance $S(f)$ is narrow-band, centered around f_c and with a bandwidth of $2W$ Hz, i.e., $S(f)=0$ when $|f \pm f_c| \geq W$. Thus, the DFT coefficients in (7) are

$$s_k = \int_{-W}^{W} S(f+f_c)G_k(f+f_c)df + \int_{-W}^{W} S(f-f_c)G_k\left(f-f_c\right)df \quad (25)$$

where

$$G_k(f) = \sum_{n=0}^{2N-1+\mu} w[n]e^{j(2\pi nf/f_s)-j(\pi n/N)k} \quad (26)$$

is a transfer function from $S(f)$ to the DFT coefficients s_k. Let $B(f)$ denote the Fourier transform of the baseband equivalent $b(t)$ from (24). Substituting $S(f)=B(f-f_c)+B^*(-f-f_c)$ in (25) yields

$$s_k = \int_{-W}^{W} B(f)G_k\left(f+f_c\right)df + \int_{-W}^{W} B^*\left(-f\right)G_k(f-f_c)df. \quad (27)$$

Applying an idea from [19] (which also considers narrow-band signals), we separate the known parts from the unknown in (25) by Taylor expanding $G_k(\cdot)$ around $\pm\widehat{f}_c$

$$G_k\left(f+\widehat{f}_c\right) = \sum_{l=0}^{L-1} \frac{f^l G_k^{(l)}\left(+\widehat{f}_c\right)}{l!} + O(f^L) \quad (28)$$

$$G_k\left(f-\widehat{f}_c\right) = \sum_{m=0}^{M-1} \frac{f^m G_k^{(m)}\left(-\widehat{f}_c\right)}{m!} + O\left(f^M\right). \quad (29)$$

Truncation of these series and insertion into (25) gives a linear approximation $\widetilde{s}_k$ of s_k

$$\begin{aligned} s_k \approx \widetilde{s}_k &\triangleq \sum_{l=0}^{L-1} G_k^{(l)}\left(+\widehat{f}_c\right)\int_{-W}^{W} B(f)\left(\frac{f^l}{l!}\right)df \\ &\quad + \sum_{m=0}^{M-1} G_k^{(m)}(-\widehat{f}_c)\int_{-W}^{W} B^*(-f)\left(\frac{f^m}{m!}\right)df \\ &= \sum_{l=0}^{L-1} c_l G_k^{(l)}\left(+\widehat{f}_c\right) + \sum_{m=0}^{M-1} d_m G_k^{(m)}(-\widehat{f}_c) \end{aligned} \quad (30)$$

where $|s_k-\widetilde{s}_k|$ represents the model error from truncation of the Taylor series and where

$$c_l = \frac{1}{l!}\int_{-W}^{W} f^l B(f)df \quad (31)$$

$$d_m = \frac{1}{m!}\int_{-W}^{W} f^m B^*(-f)df \quad (32)$$

are the unknown parameters modeling the RFI. From (32) we identify the following relation between c_m and d_m:

$$d_m = (-1)^m c_m^*. \quad (33)$$

Thus, we have the following linear model of the RFI:

$$\widetilde{s}_k = \sum_{l=0}^{L-1} c_l G_k^{(l)}\left(+\widehat{f}_c\right) + \sum_{m=0}^{M-1}(-1)^m c_m^* G_k^{(m)}(-\widehat{f}_c) \quad (34)$$

which means that we in practice have $\max(L,M)$ unknown model parameters.

We can express (34) in a matrix notation as

$$\mathbf{s} \approx \widetilde{\mathbf{s}} \triangleq \mathbf{G}\mathbf{c} \quad (35)$$

where (36), shown at the bottom of the page, holds, and

$$\mathbf{c} = \left(\begin{array}{ccccccc} c_0 & \cdots & c_{L-1} & c_0^* & \cdots & (-1)^{M-1}c_{M-1}^* \end{array}\right)^T. \quad (37)$$

When windowing is used the second sum in (34), which corresponds to the negative frequencies, gives almost no contribution to $\widetilde{s}_k$. This means that the sizes of the vector $\mathbf{c}$ and matrix $\mathbf{G}$ can be reduced to $(L\times 1)$ and $(N\times L)$, respectively.

B. Time-Domain Approach

Consider the above parameterization of the RFI. An equivalent time-domain approach is to make a Taylor series expansion of the baseband equivalent (24), $b(t)$, in the time domain. If the bandwidth of the RF signal is smaller than the inter-tone spacing of the DMT system, then the baseband function $b(t)$ will not change much within the duration of one DMT frame. Thus, we can get a good representation of $b(t)$ by a low order polynomial. We start with Taylor expanding $b(t)$ around $t=0$

$$b(t) = \sum_{k=0}^{\infty} \frac{t^k}{k!} b^{(k)}(0) \quad (38)$$

$$\mathbf{G} = \begin{pmatrix} G_0(\widehat{f}_c) & \cdots & G_0^{(L-1)}(\widehat{f}_c) & G_0(-\widehat{f}_c) & \cdots & G_0^{(M-1)}(-\widehat{f}_c) \\ \vdots & \vdots & \vdots & \vdots & \vdots & \vdots \\ G_{N-1}(\widehat{f}_c) & \cdots & G_{N-1}^{(L-1)}(\widehat{f}_c) & G_{N-1}(-\widehat{f}_c) & \cdots & G_{N-1}^{(M-1)}(-\widehat{f}_c) \end{pmatrix} \quad (36)$$

where $b^{(k)}(0)$ now represents the unknown parameters in the model. Then, the continuous time-domain RFI signal (24) can be written as

$$s(t) \approx \tilde{s}(t) = \left(\sum_{l=0}^{L-1} \frac{b^{(l)}(0)}{l!} t^l \right) e^{j2\pi f_c t} + \left(\sum_{m=0}^{M-1} \frac{b^{*(m)}(0)}{m!} t^m \right) e^{-j2\pi f_c t}. \quad (39)$$

Sampling and demodulating this RFI signal with the DFT yields

$$\widetilde{s}_k = \sum_{n=0}^{2N-1+\mu} w[n] s\left(\frac{n}{f_s}\right) e^{-j(\pi n/N)k} \quad (40)$$

$$= \sum_{l=0}^{L-1} b^{(l)}(0) \sum_{n=0}^{2N-1+\mu} \frac{\left(\frac{n}{f_s}\right)^l}{l!} w[n] e^{j(2\pi n f_c/f_s) - j(\pi n/N)k} + \sum_{m=0}^{M-1} b^{*(m)}(0) \sum_{n=0}^{2N-1+\mu} \frac{\left(\frac{n}{f_s}\right)^m}{m!} w[n] \times e^{-j(2\pi n f_c/f_s) - j(\pi n/N)k} \quad (41)$$

where $b^{(l)}(0)$ are the unknown parameters that need to be estimated, and the rest in known and does not depend on the RFI signal.

This model of the RFI is actually the same as the model in (34). The parameters in (32) are related to the parameters in (38) by

$$c_l = \frac{1}{l!} \frac{b^{(l)}(0)}{(2\pi j)^l}. \quad (42)$$

Then, by expanding the derivatives of $G_k^{(l)}(f_c)$ as

$$G_k^{(l)}(f_c) = \frac{d^l}{df^l} \left(\sum_{n=0}^{2N-1+\mu} w[n] e^{j(2\pi n f/f_s) - j(\pi n/N)k} \right)_{f=f_c} \quad (43)$$

$$= \sum_{n=0}^{2N-1+\mu} \left(j\frac{2\pi n}{f_s} \right)^l w[n] \times e^{j(2\pi n f_c/f_s) - j(\pi n/N)k} \quad (44)$$

$$= \sum_{n=0}^{2N-1+\mu} (j2\pi)^l \left(\frac{n}{f_s} \right)^l w[n] \times e^{j(2\pi n f_c/f_s) - j(\pi n/N)k} \quad (45)$$

and using this in the expression for the DFT coefficients in the model derived from the frequency-domain approach (34), we get

$$\widetilde{s}_k = \sum_{l=0}^{L-1} c_l G_k^{(l)}(+f_c) + \sum_{m=0}^{M-1} (-1)^m c_m^* G_k^{(m)}(-f_c) \quad (46)$$

$$= \sum_{l=0}^{L-1} b^{(l)}(0) \sum_{n=0}^{2N-1+\mu} \frac{\left(\frac{n}{f_s}\right)^l}{l!} w[n] e^{j(2\pi n f_c/f_s) - j(\pi n/N)k} + \sum_{m=0}^{M-1} b^{*(m)}(0) \sum_{n=0}^{2N-1+\mu} \frac{\left(\frac{n}{f_s}\right)^m}{m!} w[n] \times e^{-j(2\pi n f_c/f_s) - j(\pi n/N)k} \quad (47)$$

which is the same as we got with the time-domain approach (41).

REFERENCES

[1] K. T. Foster, "The RFI environment for VDSL," in *Proc. IEEE Globecom VDSL Workshop*, London, U.K., Nov. 1996.

[2] J. A. C. Bingham, "Multicarrier modulation for data transmission: An idea whose time has come," *IEEE Commun. Mag.*, vol. 28, pp. 5–14, May 1990.

[3] "Transmission and multiplexing (TM) access transmission systems on metallic access cables; very high speed digital subscriber line (VDSL) Part 2: Transceiver specification," ETSI, Sophia Antipolis, France, Tech. Spec. TS 101 270-2 V1.1.1 (2001-02), ETSI STC TM 6, 2001.

[4] "Very-high bit-rate digital subscriber lines (VDSL) metallic interface, Part 3: Technical specification of a multi-carrier modulation transceiver," ANSI, Vancouver, BC, Canada, Tech. Rep. T1E1.4/2002-099, 2002.

[5] J. A. C. Bingham, J. M. Cioffi, and M. Mallory, "SDMT methods of dealing with RFI,", Contribution to ETSI Sub-Technical Committee TM6, 1996.

[6] P. Ödling, P. O. Börjesson, T. Magesacher, and T. Nordström, "An approach to analog mitigation of RFI," *IEEE J. Select. Areas. Commun.*, vol. 20, pp. 974–986, June 2002.

[7] P. Spruyt, P. Reusens, and S. Braet, "Performance of improved DMT transceiver for VDSL," ANSI, Colorado Springs, CO, Tech. Rep. T1E1.4/96-l04, 1996.

[8] M. A. Soderstrand, T. G. Johnson, R. H. Strandberg, H. H. Loomis Jr, and K. V. Rangarao, "Suppression of multiple narrow-band interference using real-time adaptive notch filters," *IEEE Trans. Circuits Syst. II*, vol. 44, pp. 217–225, Mar. 1997.

[9] K. W. Martin, "Small sidelobe filter design for multitone data-communication application," *IEEE Trans. Circuits Syst. II*, vol. 45, pp. 1155–1161, Aug. 1995.

[10] J. A. C. Bingham, "RFI suppression in multicarrier transmission system," in *Proc. Globecom*, vol. 2, London, U.K., Nov. 1996, pp. 1026–1030.

[11] B. Wiese and J. Bingham, "Digital radio frequency cancellation for DMT VDSL," ANSI, Sacramento, CA, Tech. Rep. T1E1.4/97-460, 1997.

[12] T. Starr, J. M. Cioffi, and P. Silverman, *Understanding Digital Subscriber Line Technology*. Upper Saddle River, NJ: Prentice Hall, 1999.

[13] F. Sjöberg, R. Nilsson, N. Grip, P. O. Börjesson, S. K. Wilson, and P. Ödling, "Digital RFI suppression in DMT-based VDSL systems," in *Proc. Int. Conf. Telecommunications*, vol. 2, Chalkidiki, Greece, June 1998, pp. 189–193.

[14] "Transmission and multiplexing (TM); access transmission systems on metallic cables; very high speed digital subscriber line (VDSL); Part 1: Functional requirements," ETSI, Sophia Antipolis, France, Tech. Spec. TS 101 270-1 V1.2.1 (1999-10), 1999.

[15] S. Haykin, *Adaptive Filter Theory*, 3rd ed. Englewood Cliffs, NJ: Prentice Hall, 1996.

[16] L. L. Scharf, *Statistical Signal Processing: Detection, Estimation, and Time Series Analysis*. Reading, MA: Addison-Wesley, 1991.

[17] R. Nilsson, F. Sjöberg, and J. P. LeBlanc, "A rank-reduced LMMSE canceller for narrow-band interference suppression in OFDM-based systems," *IEEE Trans. Commun.*, vol. 51, pp. 2l26–2140, Dec. 2003.

[18] "Very high bit rate digital subscriber line (VDSL) metallic interface, Part 1: Functional requirements and common specification," ANSI, Vancouver, BC, Canada, Tech. Rep. T1E2.4/2002-031R2, 2002.

[19] H. Eriksson, P. O. Börjesson, P. Ödling, and N.-G. Holmer, "A robust correlation receiver for distance estimation," *IEEE Trans. Ultras. Ferroelec. Freq. Contr.*, vol. 4l, pp. 596–603, Sept. 1994.



Frank Sjöberg (S'95–M'01) was born in Umeå, Sweden, in 1970. He received the M.S. degree in computer science and the Ph.D. degree in signal Processing from Luleå University of Technology, Luleå, Sweden, in 1995, and 2000, respectively.

Between 2000 and 2002, he was with Telia Research AB, Luleå, Sweden. He is currently an Assistant Professor in the Division of Signal Processing, Luleå University of Technology. His primary research interests are statistical signal processing and digital communication, with emphasis on wireline systems.



Rickard Nilsson (S'96–M'04) was born in Umeå, Sweden, in 1971. He received the M.S.E.E. degree, the licentiate of engineering degree, and the Ph.D. degree in signal processing, from Luleå University of Technology, Luleå, Sweden, in 1996, 1999, 2002, respectively.

Between 1997 and 2001, he worked cooperatively with Telia Research AB, Luleå, Sweden, by contributing to the development and standardization of the Zipper–DMT method for very high bit rate digital subscriber lines. During the fall semester in 1999, he was a Guest Researcher at Stanford University, Stanford, CA, working on DSL algorithms and standardization. In May 2002, he joined the Telecommunications Research Center, Vienna (ftw), Austria, where he is a Senior Researcher working in the area of signal processing for broadband access. His research interests include multicarrier modulation, statistical signal processing, low-complexity algorithms, interference suppression, and synchronization.



Per Ola Börjesson (S'70–M'80–SM'01)was born in Karlshamn, Sweden, in 1945. He received the M.Sc. degree in electrical engineering and the Ph.D. degree in telecommunication theory from Lund Institute of Technology (LTH), Lund, Sweden, in 1970 and 1980, respectively, and the Docent degree in telecommunication theory, in 1983.

Between 1988 and 1998, he was a Professor of Signal Processing, Luleå University of Technology, Luleå, Sweden. Since 1998, he has been a Professor of Signal Processing, Lund University, Lund, Sweden. His primary research interest lies in high-performance communication systems, in particular, high data rate wireless and twisted pair systems. He is presently involved in research on signal processing techniques in communication systems that use orthogonal frequency division multiplexing or discrete multitone modulation. He emphasizes the interaction between models and real systems, from the creation of application-oriented models based on system knowledge to the implementation and evaluation of algorithms.

Per Ödling (S'90–M'00–SM'01) was born in Örnsköldsvik, Sweden, in November 1966. He received the M.S.E.E., the licentiate of engineering, and the Ph.D. degrees in signal processing from Luleå University of Technology, Luleå, Sweden, in 1989, 1993, and 1995, respectively, and the Docent degree from Lund Institute of Technology, Lund, Sweden, in 2000.

From 1995 to 1999, he was an Assistant Professor at Luleå University of Technology, advising graduate students, teaching, managing a large research cooperation with Telia Research AB, and as Vice Head of the Division of Signal Processing. At the same time, he consulted for Telia Research AB, Luleå, Sweden, and STMicroelectronics, Toulouse, France, developing an OFDM-based proposal for the standardization of IMT-2000/UMTS. He also developed very high bit rate digital subscriber line modems for standardization in ITU, ETSI, and ANSI. In 1999, he joined the Telecommunications Research Center, Vienna, Austria, where he spent three years advising graduate students and industry, while researching broadband Internet access and services. While in Vienna, he consulted for the Austrian Telecommunications Regulatory Authority on the technical impact of the unbundling of the local loop. In 2003, he was appointed Full Professor of Telecommunications, Lund Institute of Technology, and has been since 2003, stationed at Ericsson Telecom AB, Stockholm, as a part of a cooperation. He is currently developing broadband communication systems for Internet access over radio and twisted copper pairs, and advises Ph.D. students in these areas. His research interests focus on signal processing and statistical communications, but range to the convergence of data- and telecommunications and technical regulatory issues. He has published more than forty journal and conference papers, thirty-five standardization contributions, and a dozen patents.

Dr. Ödling also serves as an Associate Editor for the IEEE TRANSACTIONS ON VEHICULAR TECHNOLOGY.

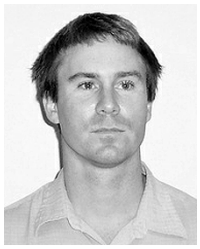

Brian Wiese received B.S. degrees in electrical engineering and physics from California State University, Chico, CA, in 1995, and the M.S. degree in electrical engineering from Stanford University, Stanford, CA, in 1997.

He joined Amati Communications (now Texas Instruments), Dallas, TX, in 1996, where he was a primary DSP designer of asymmetrical digital subscriber lines (ADSL) and very high bit rate digital subscriber line hardware and software. Since February 2004, he has been with 2Wire Incorporated, San Jose, CA as a Senior DSP Engineer. He holds three US Patents and has written articles for IEEE COMMUNICATIONS MAGAZINE and IEEE JOURNAL ON SELECTED AREAS IN COMMUNICATIONS.



John A. C. Bingham (M'59–SM'68–F'93–LF'99) now retired, worked for 40 years in the San Francisco Bay area mostly in data communication, and the last five years with Amati (now part of Texas Instruments), Dallas, TX, helping to invent digital subscriber lines. He was the Editor of the *U.S. Standard on DSL*, and is the author of two books on data transmission.